JOURNAL OF THEORETICAL
AND APPLIED MECHANICS
63, 3, pp. 525–534, Warsaw 2025
https://doi.org/10.15632/jtam-pl/202293

EVALUATION OF SHAPE TRANSFORMATION IN 4D PRINTED POLYLACTIC ACID USING COPPER WIRES

Raul-Mihai PETRAȘCU*, Sever-Gabriel RACZ, Eugen AVRIGEAN

Department of Industrial Machines and Equipment, Engineering Faculty, Lucian Blaga University of Sibiu, Sibiu 550025, Romania

*corresponding author, *raul.petrascu@ulbsibiu.ro*

This study explores the shape transformation of 4D printed polylactic acid (PLA) specimens activated by thermal stimulation above the glass transition temperature (T_g). Two methods were explored: (1) triggering shape transformation in a rectangular prism, "Flower", and "Spiderweb" designs via hot water immersion; and (2) inducing shape transformation through Joule heating using copper wires.

Keywords: polylactic acid; 4D printing; Joule heating; shape transformation; shape memory polymers.

1. Introduction

Fused filament fabrication (FFF), an extension of fused deposition modeling (FDM), is a 3D printing technique that builds objects layer-by-layer while extruding a semiliquid material through a nozzle (Ree, 2024). Material extrusion, or MEX, is a method that supports various thermoplastics, typically in the form of filaments. Polylactic acid (PLA) is biocompatible, ideal for usage in medical applications (DeStefano *et al.*, 2020), and biodegradable, which enables the development of environmentally friendly blends (Yousefi *et al.*, 2024).

Tibbits (2014) introduced the concept of 4D printing, which involves creating structures that modify their properties in response to external stimuli such as heat, light, magnetic fields, or pH changes. Smart materials which interact with stimuli can expand, contract, self-assemble, or self-heal, resulting in movements or structural adaptations (Petrașcu *et al.*, 2023). Shape memory polymers (SMPs) are of interest due to their shape memory effect (SME). The SME in SMPs refers to a material's ability to recover or transform into a programmed shape.

In 3D printing, a PLA sample is programmed for shape transformation after fabrication. The sample temperature (T_s) is raised above its glass transition temperature (T_g), which typically ranges from 44 °C to 63 °C (Crawford & Quinn, 2017). Above T_g, the material softens, which allows it to be deformed under an applied load into an intermediate shape. Under normal conditions, the sample retains this new shape due to the viscoelastic properties of the polymer until it is reheated above T_g, which triggers recovery to its programmed geometry, thus completing the SME cycle (Riley *et al.*, 2020).

Ministry of Science and Higher Education
Republic of Poland

The publication has been funded by the Polish Ministry of Science and Higher Education under the Excellent Science II programme "Support for scientific conferences".
The content of this article was presented during the 40th Danubia-Adria Symposium on Advances in Experimental Mechanics, Gdańsk, Poland, September 24–27, 2024.

In 4D printing, PLA sample programming is determined by printing parameters. The printed sample is considered an intermediate shape until T_s exceeds T_g, triggering the transformation into the programmed shape (Hosseinzadeh *et al.*, 2023). This transformation is driven by residual strain accumulated during the 3D printing process, influenced by temperature gradients and cooling rates. By adjusting printing parameters, such as printing speed, layer thickness and printing temperature, the amount of residual strain can be controlled (Wang & Li, 2020; Wu *et al.*, 2022). Figure 1 illustrates these programming approaches.

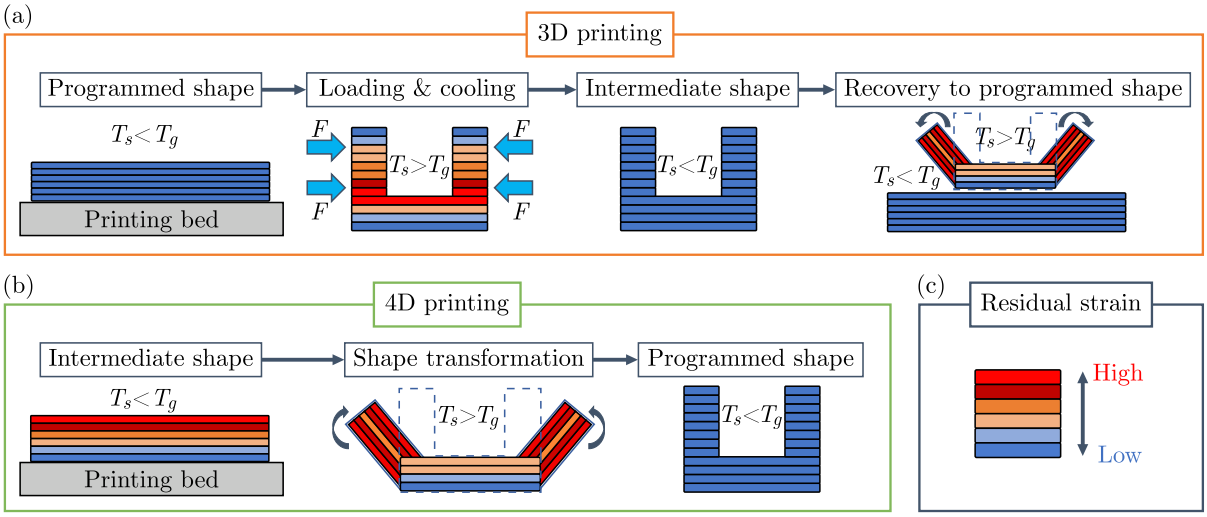

Fig. 1. Shape memory effect (SME): (a) 3D printing; (b) 4D printing; (c) residual strain levels [adapted from (Hosseinzadeh *et al.*, 2023)].

The activation of SME in PLA has been studied using various methods, including infrared radiation (Ren *et al.*, 2023), hot water immersion (Mehrpouya *et al.*, 2021), and conductive heating with resistive fillers like carbon black (Liu *et al.*, 2024), carbon nanotubes (Gholizadeh Ledari & Zolfaghari, 2025), and metal particles (Shao *et al.*, 2020). These fillers often require high voltage inputs; for example, Liu *et al.* (2019) used 70 V to activate a PLA-based gripper with carbon nanotubes.

Since higher filler content raises viscosity and necessitates more intensive mixing (Zhu *et al.*, 2021), its use presents challenges such as complex material preparation requiring uniform dispersion and strong interfacial bonding within the polymer matrix, as well as increased energy demands (Wang *et al.*, 2021). Moreover, PLA is inherently brittle, exhibits poor impact resistance, low heat tolerance, and limited dimensional stability at high temperatures (Wang *et al.*, 2024). To address these limitations, this study explores a simple and cost-effective approach to inducing shape transformation in 4D printed PLA specimens by embedding copper wires. Thermal activation above the T_g is applied in two ways: (1) in a water environment, where embedded copper wires control bending while mitigating the degradation of PLA's mechanical properties over time, and (2) in a non-fluid environment, where Joule heating of the embedded wires activates shape transformation.

The paper is structured as follows: Section 2 describes the sample design, printing parameters, and experimental setups for thermal stimulation using hot water immersion and Joule heating. It also details two configurations for embedding copper wires. Section 3 presents and discusses the results, starting with PLA's shape transformation in hot water, followed by the effects of embedded copper wires through Joule heating. Additionally, energy consumption is compared between configurations. Finally, Section 4 summarizes the study's findings.

2. Experimental section

2.1. Materials

Specimens were 3D printed using the FFF technique on an Ultimaker Connect 2+ 3D printer. The sample design is shown in Figs. 2a and 2c, with the corresponding printing parameters (Fig. 2b). Bell-shaped holes (Fig. 2d) were integrated to enable the post-printing insertion of copper wires. Two PLA filaments (2.85 mm diameter) were tested: red (Copper 3D) and blue (Ultimaker).

(a)

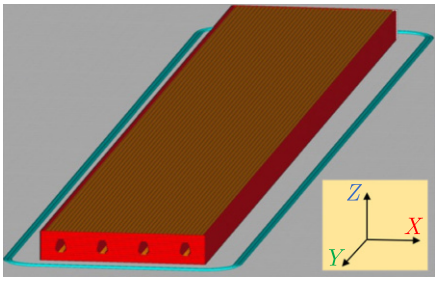

(b)

Printing speed	80 mm/s
Nozzle diameter	0.4 mm
Nozzle temperature	190 °C
Layer thickness	0.1 mm
Bed temperature	0 °C
Infill density	100 %
Infill line directions	first ×4 layers = 90° rest ×11 layers = 0°

(c)

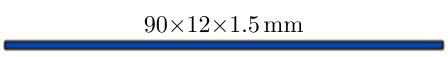

(d)

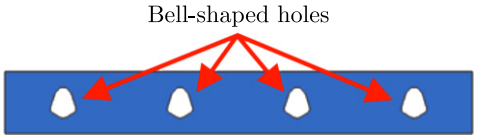

Fig. 2. Sample design: (a) isometric view; (b) printing parameters; (c) lateral view, sample dimensions in millimeters, scale 1:2; (d) front view, bell-shaped holes, scale 1:16.

2.2. Testing procedure

Figure 3 presents the experimental setups designed to activate the shape transformation of PLA specimens in two different scenarios. In the first setup, specimens were immersed in hot water, with temperature regulated using a Zilan ZLN 4007 device, which employs a pump for fluid recirculation and a thermoplunger for heating. In the second setup, copper wires were embedded in the specimens and connected to a power supply delivering a constant 5 A current.

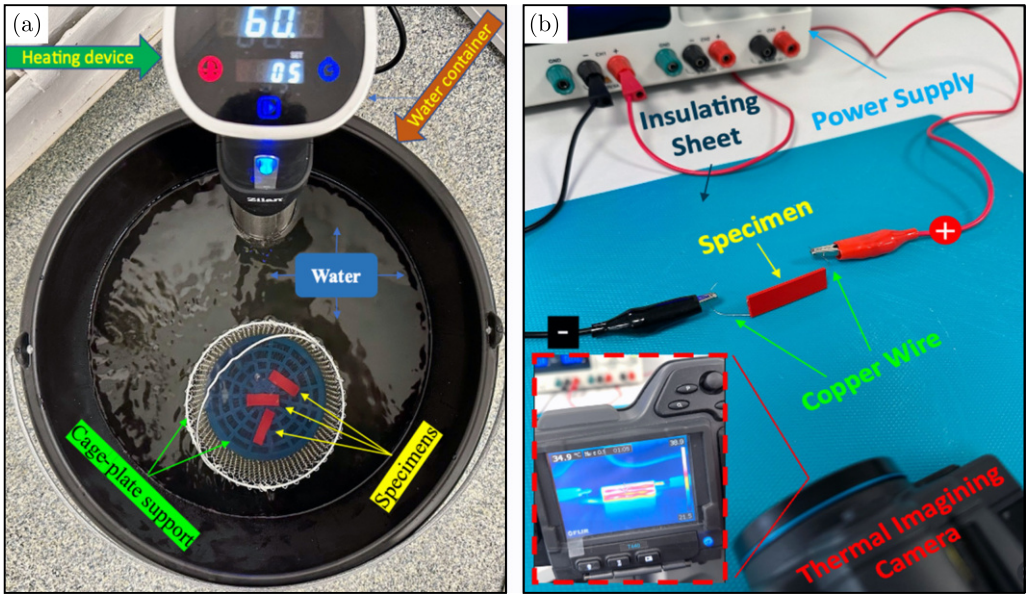

Fig. 3. Experimental setups: (a) immersion in hot water; (b) Joule heating.

Due to copper's negligible resistance, only the current required regulation. The temperature was monitored using a FLIR T440 thermal imaging camera.

The wire configurations are illustrated in Fig. 4. In the parallel configuration, four separate 100 mm wires were inserted individually, whereas the series configuration utilized a single continuous 400 mm wire. In both setups, after fabrication, 0.2 mm diameter copper wires were integrated into the specimens through bell-shaped holes.

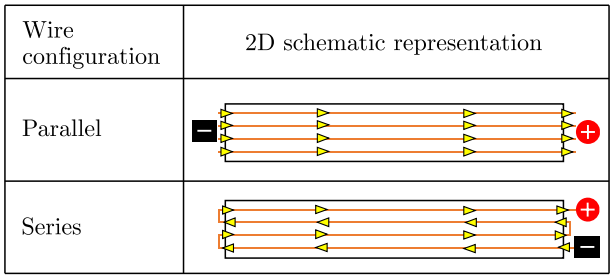

Fig. 4. 2D schematic of wire configurations and current flow pathways within the specimens.

3. Results and discussion

3.1. Shape transformation via hot water immersion

The first part of the study involves immersing 4D printed PLA specimens in hot water, which is a widely used method for activating shape transformation. Figure 5 illustrates the specimens' response in a water environment, where initially flat PLA samples undergo self-bending. At 65 °C, both specimens exhibit noticeable bending, while at 75 °C and 85 °C, they form coiled shapes. Notably, the red sample self-bends consistently, whereas the blue sample displays asymmetrical self-bending, likely due to variations in residual strain and filament color. The filament color affects PLA's thermal properties, while printing temperature plays a key role in achieving high crystallinity, which is essential for multiple SME cycles (Frunzaverde *et al.*, 2023; Cadete *et al.*, 2025).

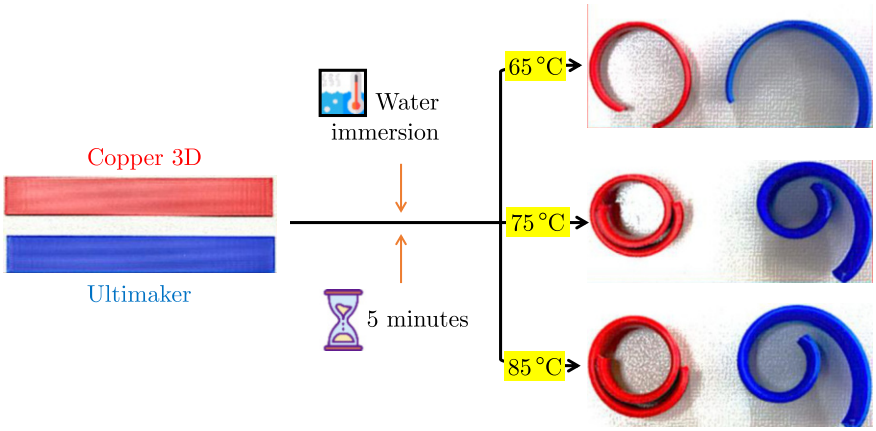

Fig. 5. Self-bending response of PLA specimens immersed in water at different temperatures.

The study further examines the shape transformations of PLA in hot water, focusing on more complex geometries. Figure 6 illustrates flat specimens transforming into concave, petal-like shapes when immersed at 70 °C. Similarly, Fig. 7 shows a spiderweb-shaped specimen undergoing the same transformation.

Figure 8 illustrates the self-bending deformation of 4D printed PLA specimens both without embedded wires (S_x) and with wires having a diameter of 0.2 mm (S_{02}), arranged in a parallel configuration.

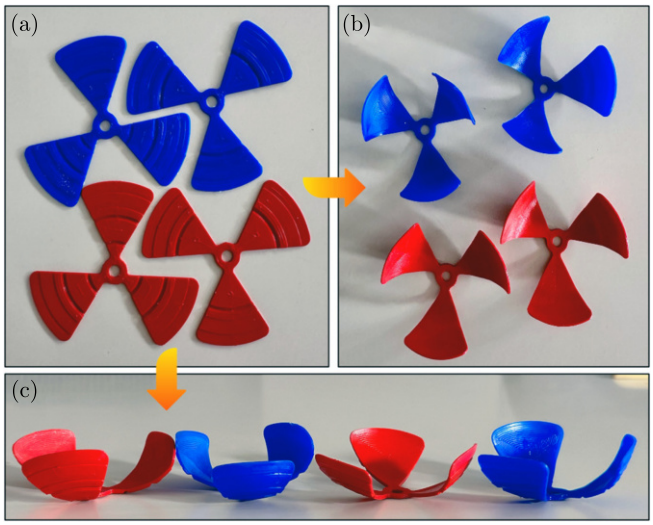

Fig. 6. Shape transformation of flower-shaped specimens: (a) 3D printed parts; (b) front view after thermal activation; (c) perspective view after thermal activation.

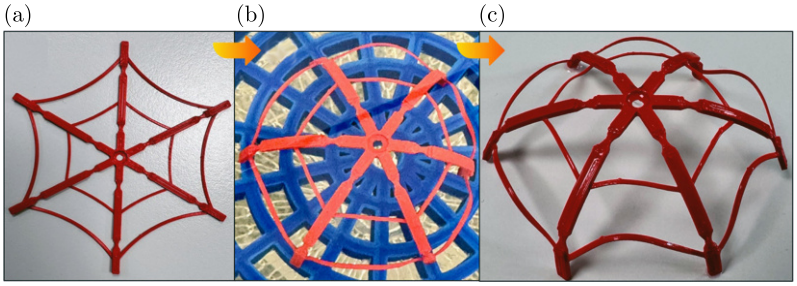

Fig. 7. Spiderweb sample shape transformation: (a) 3D printed part; (b) immersion in hot water; (c) perspective view after thermal activation.

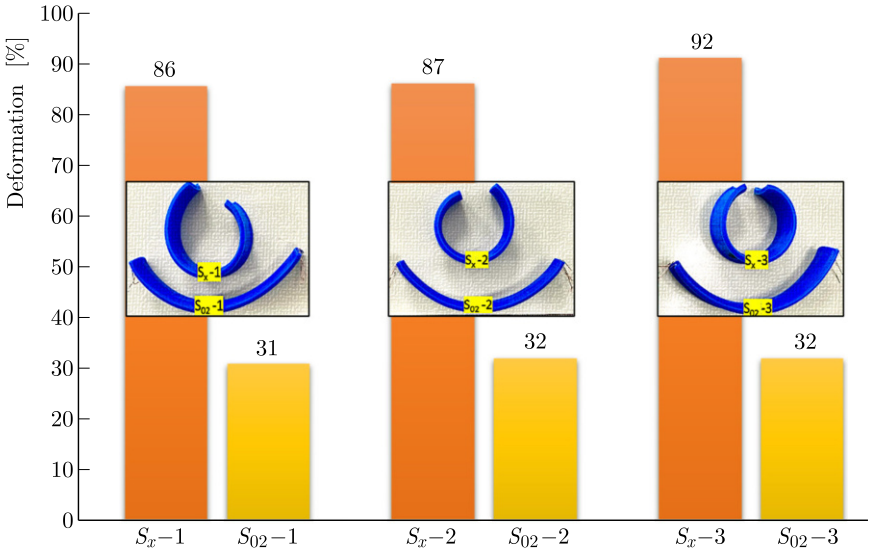

Fig. 8. Comparison of self-bending between specimens without integrated wires (S_x) and specimens with integrated copper wires (S_{02}).

The self-bending (S_b) for each specimen was calculated using Eq. (3.1), where L_0 represents the initial length and L_f the final length. Specimens without wires exhibited an average bending deformation of 88 %, consistent with findings by Ansaripour *et al.* (2024). In contrast, specimens with embedded copper wires exhibited a bending deformation of 56 %, reflecting a 32 % reduc-

tion. Each embedded wire contributed to an 8 % decrease in self-bending, indicating that copper wires can be utilized for controlled bending:

$$S_b = \frac{L_f - L_0}{L_0} \times 100. \tag{3.1}$$

Mechanical tests from the literature typically show a slight decline in material properties after multiple cycles of deformation and recovery (Ehrmann & Ehrmann, 2021). In this context, embedded wires can help preserve mechanical properties. In semi-crystalline PLA, heating times influence crystallinity when temperatures exceed T_g, with higher crystallinity enhancing shape fixity and recovery. This process is crucial for repeated deformation and recovery cycles, as it forms ordered, spring-like structures that interconnect polymer chains. However, over time, PLA can achieve sufficient crystallization through heat treatment (e.g., annealing), and this eliminates the need for further crystallization (Da Cunha *et al.*, 2023). Additionally, prolonged immersion in water allows PLA to absorb moisture due to its hydrophilic nature, which acts as a plasticizer, increasing macromolecular flexibility and lowering T_g, thereby facilitating shape recovery (Zhang *et al.*, 2020). These factors highlight the complex interplay between heat, environmental conditions, and PLA's shape memory response.

3.2. Shape transformation through Joule heating

3.2.1. Parallel configuration

In the first Joule heating scenario, four copper wires were embedded into a 3D printed sample (Fig. 2) in a parallel configuration (Fig. 4) and connected to a DC power source, supplying 5 A. Temperature measurements were recorded every 15 seconds for up to 60 seconds, as shown in Fig. 9. The results show a temperature increase from 26.4 °C to 33.3 °C over the entire interval, with a total rise of approximately 7 °C. Even so, since the internal temperature did not reach the T_g range, no shape transformation occurred. The highest temperature was recorded at the positive terminal due to electron accumulation at the circuit's exit, while the outer wires exhibited lower heating efficiency due to heat dissipation into the environment. However, reducing the wire length could enhance heating efficiency, making this setup more suitable for localized heating applications.

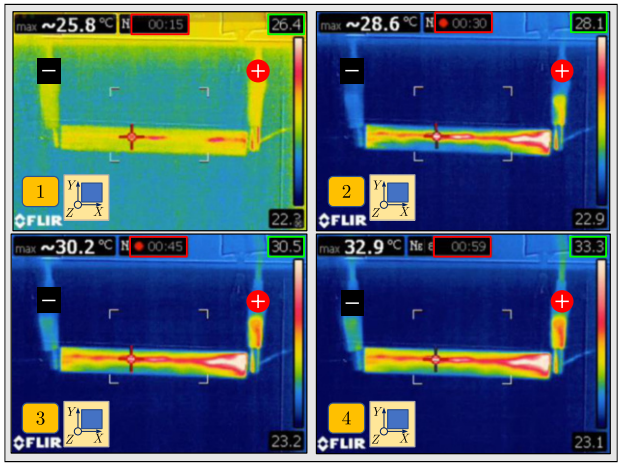

Fig. 9. Monitoring the temperature in parallel wires configuration.

3.2.2. Series configuration

In the second Joule heating scenario, a single copper wire was embedded into a 3D printed sample (Fig. 2) in a series configuration (Fig. 4) and connected to a DC power source, supplying 5 A. Temperature values recorded during the test are shown in Fig. 10. The results

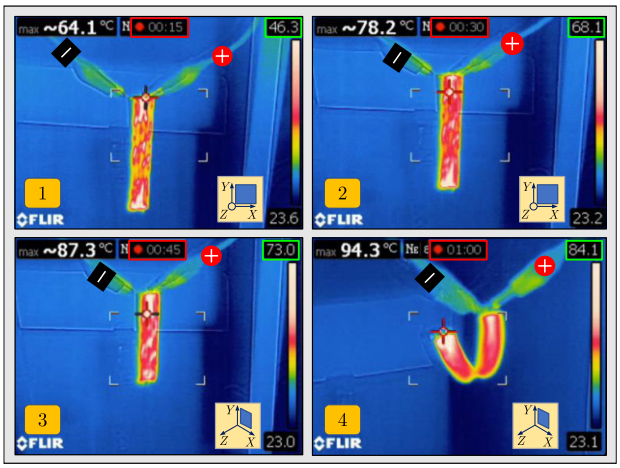

Fig. 10. Monitoring the Joule heating effect applied by integration of a single continuous copper wire.

indicate a faster temperature increase, from 46.3 °C to 84.1 °C, with a total increase of approximately 38 °C within 60 seconds. The highest temperatures were observed at the sample's ends, where the wire changed direction, leading to increased electron collisions.

In the first 15 seconds, the temperature reached 46.3 °C, which is below the T_g range of PLA and thus prevents any transformation. By 30 seconds, the temperature rose to 68.1 °C, surpassing T_g; however, the material's response was delayed. At 45 seconds, the temperature reached 73 °C, causing the unattached end of the sample to begin bending, which prompted a slight camera adjustment to capture the movement. By 60 seconds, the temperature reached approximately 84 °C, and the bending became more pronounced, with heat distribution appearing symmetrical within the sample.

Based on these findings, the series configuration may be effective for gripping applications. A similar study by (Shao *et al.*, 2020) used copper wires for localized heat transfer to activate a biomimetic flower-shaped gripper.

Figure 11 illustrates the energy consumption over time for both parallel and series configurations. The results indicate an estimated power dissipation of approximately 5.35 W. Since

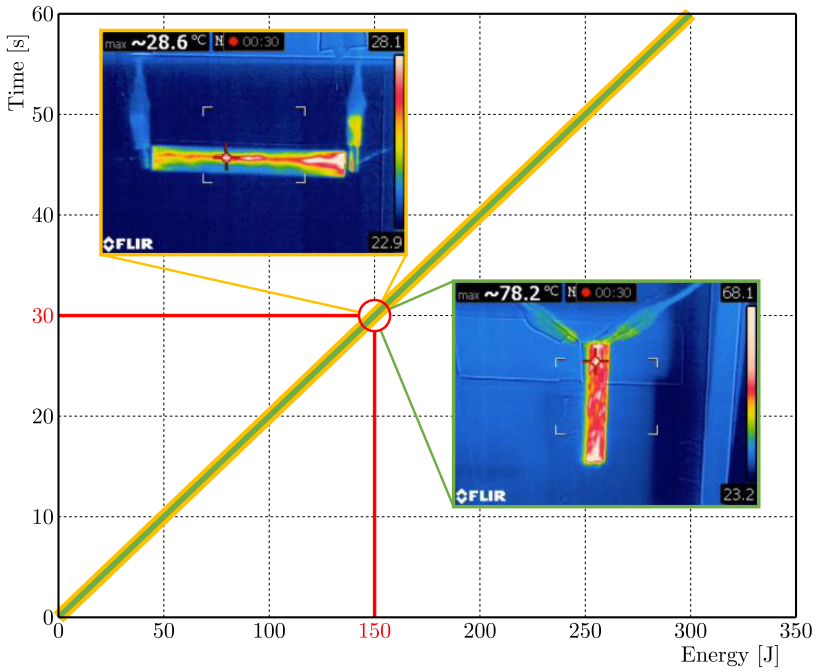

Fig. 11. Energy consumption over time for parallel and series configurations.

power directly influences the heating rate, the energy transferred increased linearly over time, reaching approximately 160 J at 30 seconds and peaking at 321 J by the end of the interval.

The inset thermal images highlight the differences in temperature distribution between the configurations. The parallel setup reached 28.6 °C, while the series configuration attained a significantly higher value 78.2 °C. In contrast, studies utilizing conductive composites typically require higher voltages, up to 60 V (Liu *et al.*, 2024) and 70 V (Liu *et al.*, 2019), due to their higher electrical resistance, which restricts current flow and reduces heating efficiency.

4. Conclusions

This study explores the shape transformation of 4D printed polylactic acid (PLA) specimens activated by thermal stimulation above the glass transition temperature (T_g) by two methods. The key findings:

1) Hot water immersion: 4D printed PLA specimens, including rectangular prism, "Flower", and "Spiderweb" designs, exhibited shape transformation in hot water, highlighting potential applications in biomedical engineering and environmental science (Da Cunha *et al.*, 2023). Additionally, embedding copper wires in rectangular prisms can help control bending, and may mitigate the degradation of PLA's mechanical properties over time.
2) Joule heating: Two wire configurations were tested in a rectangular prism sample: parallel, where separate wires were embedded, and series, where a single wire traversed the entire structure. A 5 A current was applied for 60 seconds, generating heat through Joule heating. The parallel configuration did not generate enough heat to induce shape transformation, as it required more time to reach the necessary temperature. Thus, this configuration may be suitable only with a reduced wire length, and so it is potentially useful for localized heating. In contrast, the series configuration produced bending similar to that observed in hot water, thus highlighting its potential for actuation applications such as gripping.

Further research should examine the mechanical properties after multiple SME cycles, test different wiring setups, and explore various wire material combinations. Additionally, localized heating using embedded wires could enable controlled shape transformation in specific areas.

Acknowledgments

The work was supported by the Learn. Inc 2021-1-RO01-KA220-HED-000031136 project.

References

1. Ansaripour, A., Heidari-Rarani, M., Mahshid, R., & Bodaghi, M. (2024). Influence of extrusion 4D printing parameters on the thermal shape-morphing behaviors of polylactic acid (PLA). *The International Journal of Advanced Manufacturing Technology*, *132*(3–4), 1827–1842. https://doi.org/10.1007/s00170-024-13470-6

2. Cadete, M.S., Gomes, T.E.P., Gonçalves, I., & Neto, V. (2025). Influence of 3D-printing deposition parameters on crystallinity and morphing properties of PLA-based materials. *Progress in Additive Manufacturing*, *10*(1), 127–137. https://doi.org/10.1007/s40964-024-00608-x

3. Crawford, C.B., & Quinn, B. (2017). *Physiochemical properties and degradation*. In Microplastic pollutants, (pp. 57–100). Elsevier. https://doi.org/10.1016/B978-0-12-809406-8.00004-9

4. Da Cunha, R.B., Pê, F.R., Agrawal, P., de Figueiredo Brito, G., & de Mélo, T.J.A. (2023). Influence of crystallization on the shape memory effect of poly (lactic acid). *Smart Materials and Structures*, *32*(8), 085016. https://doi.org/10.1088/1361-665X/ace226

5. DeStefano, V., Khan, S., & Tabada, A. (2020). Applications of PLA in modern medicine. *Engineered Regeneration*, *1*, 76–87. https://doi.org/10.1016/j.engreg.2020.08.002

6. Ehrmann, G., & Ehrmann, A. (2021). 3D printing of shape memory polymers. *Journal of Applied Polymer Science*, *138*(34), Article 50847. https://doi.org/10.1002/app.50847

7. Frunzaverde, D., Cojocaru, V., Bacescu, N., Ciubotariu, C.-R., Miclosina, C.-O., Turiac, R.R., & Marginean, G. (2023). The influence of the layer height and the filament color on the dimensional accuracy and the tensile strength of FDM-printed PLA specimens. *Polymers*, *15*(10), Article 2377. https://doi.org/10.3390/polym15102377

8. Gholizadeh Ledari, R., & Zolfaghari, A. (2025). 4D printing with the assistance of electrical stimulation on polylactic acid coated with carbon nanotubes. *Rapid Prototyping Journal*, *31*(4). https://doi.org/10.1108/RPJ-06-2024-0238

9. Hosseinzadeh, M., Ghoreishi, M., & Narooei, K. (2023). 4D printing of shape memory polylactic acid beams: An experimental investigation into FDM additive manufacturing process parameters, mathematical modeling, and optimization. *Journal of Manufacturing Processes*, *85*, 774–782. https://doi.org/10.1016/j.jmapro.2022.12.006

10. Liu, D., Zhu, L., Zhou, J., Xie, Y., Luo, X., & Evsyukov, S.A. (2024). Preparation and 3D printing parameters of thermo/electrically shape memory PLA/SEBS-g-MA/CB composites. *Polymer*, *313*, Article 127718. https://doi.org/10.1016/j.polymer.2024.127718

11. Liu, Y., Zhang, F., Leng, J., Fu, K., Lu, X.L., Wang, L., Cotton, C., Sun, B., Gu, B., & Chou, T. (2019). Remotely and sequentially controlled actuation of electroactivated carbon nanotube/shape memory polymer composites. *Advanced Materials Technologies*, *4*(12), Article 1900600. https://doi.org/10.1002/admt.201900600

12. Mehrpouya, M., Vahabi, H., Janbaz, S., Darafsheh, A., Mazur, T.R., & Ramakrishna, S. (2021). 4D printing of shape memory polylactic acid (PLA). *Polymer*, *230*, Article 124080. https://doi.org/10.1016/j.polymer.2021.124080

13. Petrașcu, R.M., Racz, S.-G., & Rusu, D.-M. (2023). Mapping smart materials' literature: An insight between 1990 and 2022. *Sustainability*, *15*(20), Article 15143. https://doi.org/10.3390/su152015143

14. Ree, B.J. (2024). Critical review and perspectives on recent progresses in 3D printing processes, materials, and applications. *Polymer*, *308*, Article 127384. https://doi.org/10.1016/j.polymer.2024.127384

15. Ren, L., Wang, Z., Ren, L., Liu, Q., Li, W., Song, Z., Li, B., Wu, Q., & Zhou, X. (2023). 4D printing of shape memory composites with remotely controllable local deformation. *Materials Today Chemistry*, *29*, Article 101470. https://doi.org/10.1016/j.mtchem.2023.101470

16. Riley, K.S., Ang, K.J., Martin, K.A., Chan, W.K., Faber, J.A., & Arrieta, A.F. (2020). Encoding multiple permanent shapes in 3D printed structures. *Materials & Design*, *194*, Article 108888. https://doi.org/10.1016/j.matdes.2020.108888

17. Shao, L.-H., Zhao, B., Zhang, Q., Xing, Y., & Zhang, K. (2020). 4D printing composite with electrically controlled local deformation. *Extreme Mechanics Letters*, *39*, Article 100793. https://doi.org/10.1016/j.eml.2020.100793

18. Tibbits, S. (2014). 4D printing: Multi-material shape change. *Architectural Design*, *84*(1), 116–121. https://doi.org/10.1002/ad.1710

19. Wang, X., Huang, L., Li, Y., Wang, Y., Lu, X., Wei, Z., Mo, Q., Zhang, S., Sheng, Y., Huang, C., Zhao, H., & Liu, Y. (2024). Research progress in polylactic acid processing for 3D printing. *Journal of Manufacturing Processes*, *112*, 161–178. https://doi.org/10.1016/j.jmapro.2024.01.038

20. Wang, Y., Desroches, G.J., & Macfarlane, R.J. (2021). Ordered polymer composite materials: challenges and opportunities. *Nanoscale*, *13*(2), 426–443. https://doi.org/10.1039/D0NR07547G

21. Wang, Y., & Li, X. (2020). An accurate finite element approach for programming 4D-printed self-morphing structures produced by fused deposition modeling. *Mechanics of Materials*, *151*, Article 103628. https://doi.org/10.1016/j.mechmat.2020.103628

22. Wu, P., Yu, T., Chen, M., & Hui, D. (2022). Effect of printing speed and part geometry on the self-deformation behaviors of 4D printed shape memory PLA using FDM. *Journal of Manufacturing Processes*, *84*, 1507–1518. https://doi.org/10.1016/j.jmapro.2022.11.007

23. Yousefi, M.A., Rahmatabadi, D., Baniassadi, M., Bodaghi, M., & Baghani, M. (2024). 4D printing of multifunctional and biodegradable PLA-PBAT-Fe_3O_4 nanocomposites with supreme mechanical and shape memory properties. *Macromolecular Rapid Communications*, *46*(2), Article 2400661. https://doi.org/10.1002/marc.202400661

24. Zhang, X.-J., Yang, Q.-S., Liu, X., Shang, J.-J., & Leng, J.-S. (2020). Atomistic investigation of the shape-memory effect of amorphous poly(*L*-lactide) with different molecular weights. *Smart Materials and Structures*, *29*(1), Article 015040. https://doi.org/10.1088/1361-665X/ab471c

25. Zhu, J., Abeykoon, C., & Karim, N. (2021). Investigation into the effects of fillers in polymer processing. *International Journal of Lightweight Materials and Manufacture*, *4*(3), 370–382. https://doi.org/10.1016/j.ijlmm.2021.04.003

Manuscript received December 5, 2024; accepted for publication February 24, 2025; published online May 14, 2025.